

BME 281L Lab 5: Combined Loading Using Finite Element Analysis Software

Aaren Arasaratnam

Jamie Kang

Emija Ravindran

I. Introduction

More often than not, real-world objects deal with multiple stresses at any given time. A combination of axial/shear forces, and torsional/bending moments are present in the everyday objects we use. Consequently, engineers should be able to evaluate the stress-state of a member under multiple conditions using the superposition principle, which describes the summative nature of stresses and strains on the same axes. Members are typically able to experience multiple different forces and moments at the same time, where the analysis of these forces become necessary to understand engineering designs. Combined loading is applicable anywhere and everywhere, including the shaft of a helicopter rotor or the torsional moment on the 1-bit of a surgical drill.

The objective of this is to make use of the finite element analysis (FEA) software, Abaqus [1], to model parts and materials in a simulation manner. Conditions can be defined and changed under the guidance of the user, from which the software applies mathematical formulas to analyze the behaviour at infinitesimally small points (viz., elements) which can be added up to form an accurate understanding of the behaviour of the entire part. A pre-lab was conducted prior to the study where the normal stress (N), shear (V), moment (M) and torque (T) were calculated, which were used to determine the state stresses at different points. The results from the pre-lab were hand calculated, and compared to the results given by Abaqus [1] to verify accuracy. It can be hypothesised that the hand-calculated results and the results obtained from the finite element analysis software, Abaqus, would be similar.

II. Results

1.

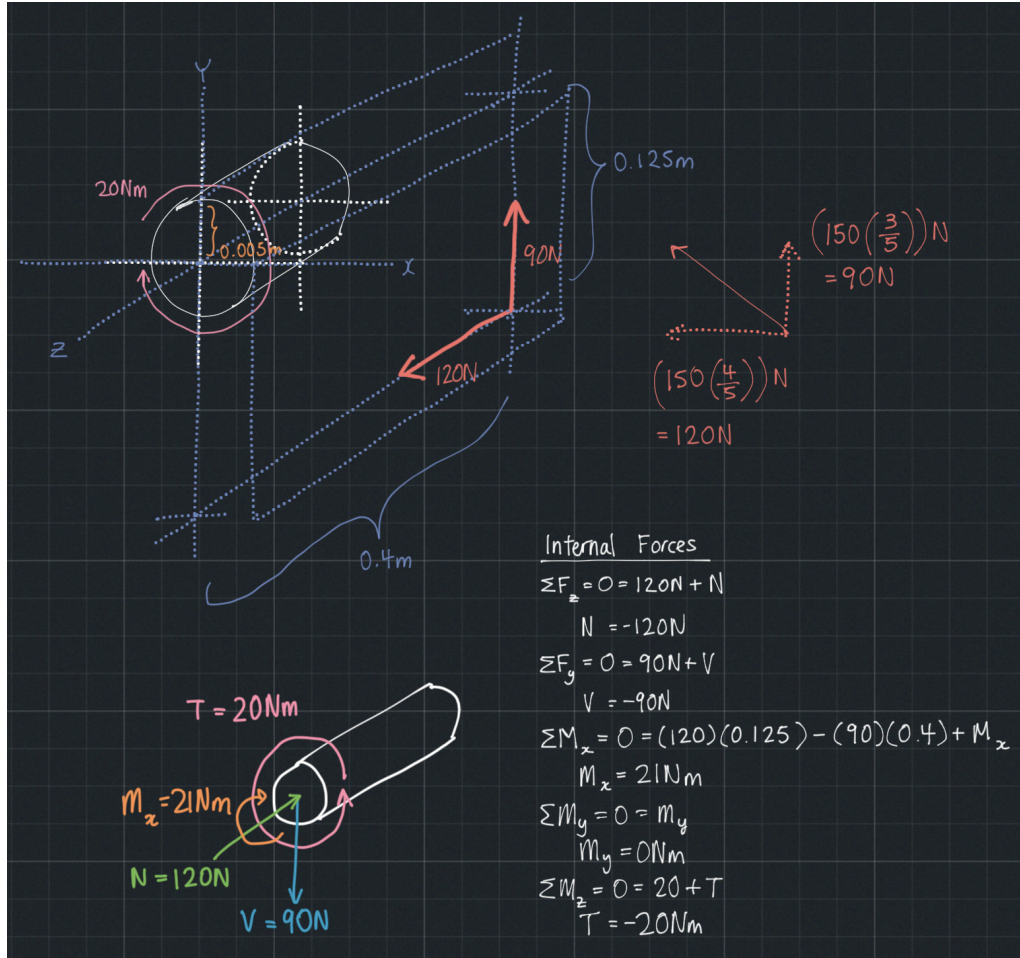


Fig. 1. Hand calculations for N , V , T , and M with an accompanying free-body diagram.

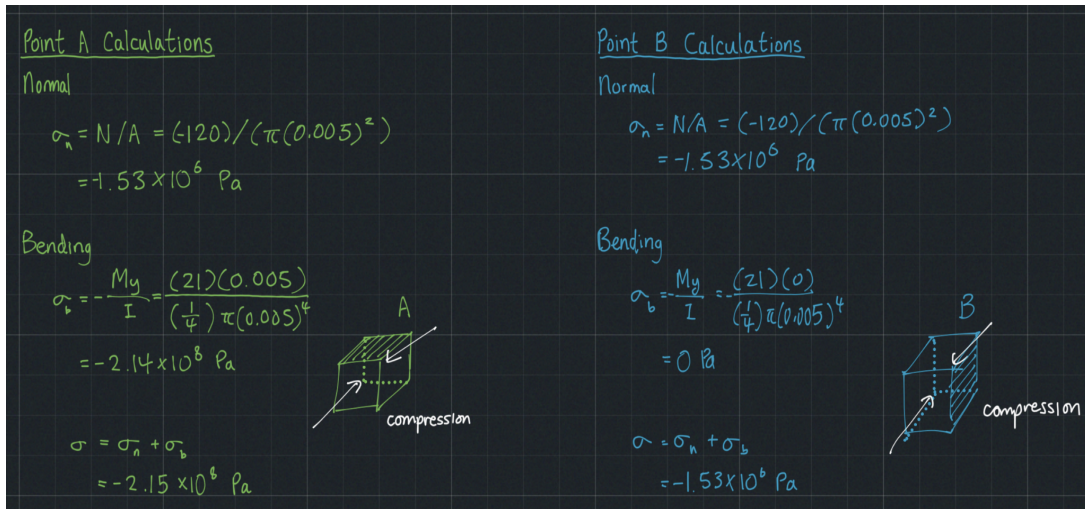
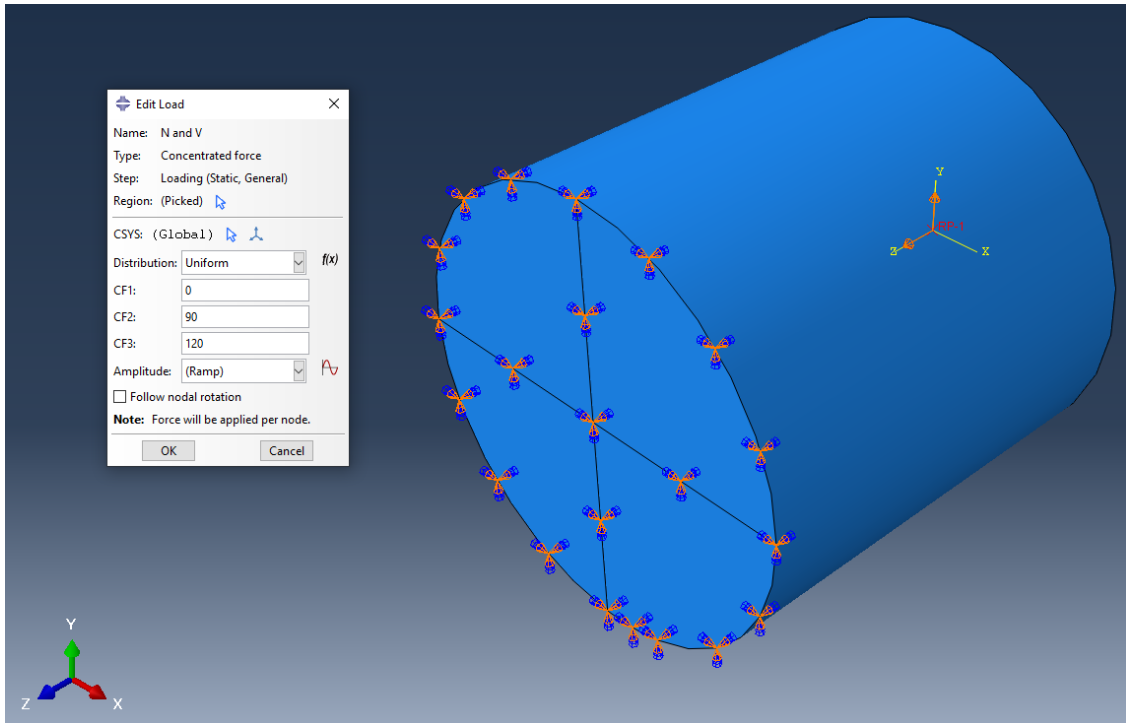


Fig. 2. Hand calculations for stresses at points A and B.

Table 1. Hand-Calculated Force and Stress Values at Points A and B

	<i>N</i>	<i>V</i>	<i>T</i>	<i>M</i>	Stress
Point A	-120 N	-90 N	-20 Nm	21 Nm	-2.15×10^8 Pa
Point B					-1.53×10^6 Pa

2.

Fig. 3. Load setting for *N* and *V* [1].

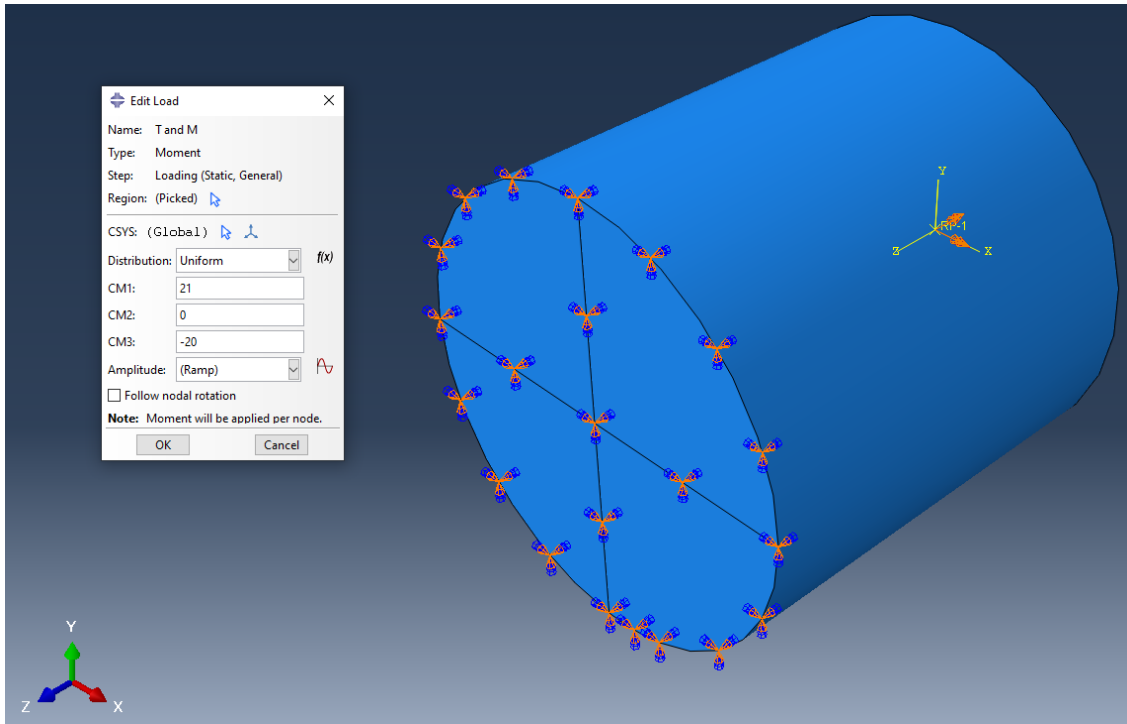


Fig. 4. Load setting for T and $V[1]$.

3.

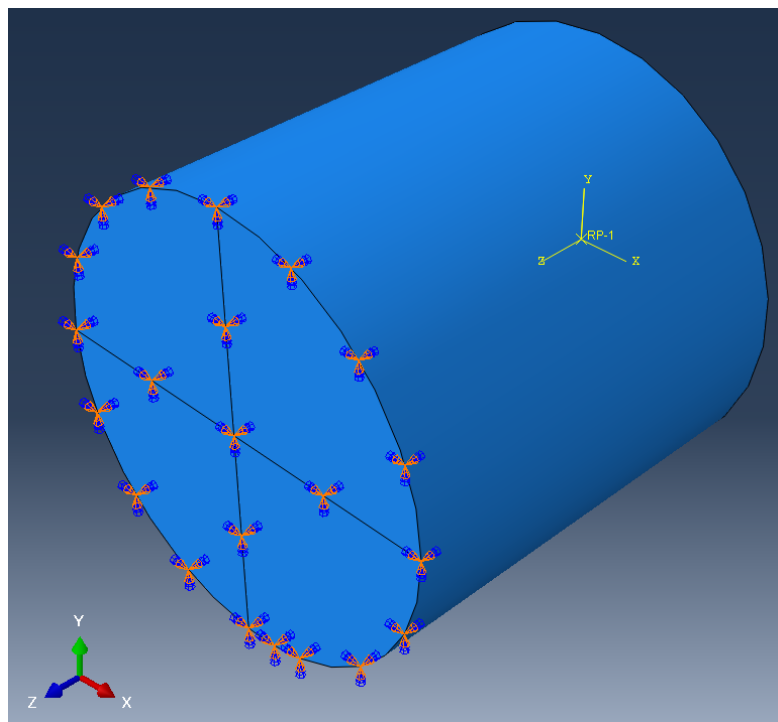


Fig. 5. Fixed face of cylinder with Boundary Condition arrows [1].

4.

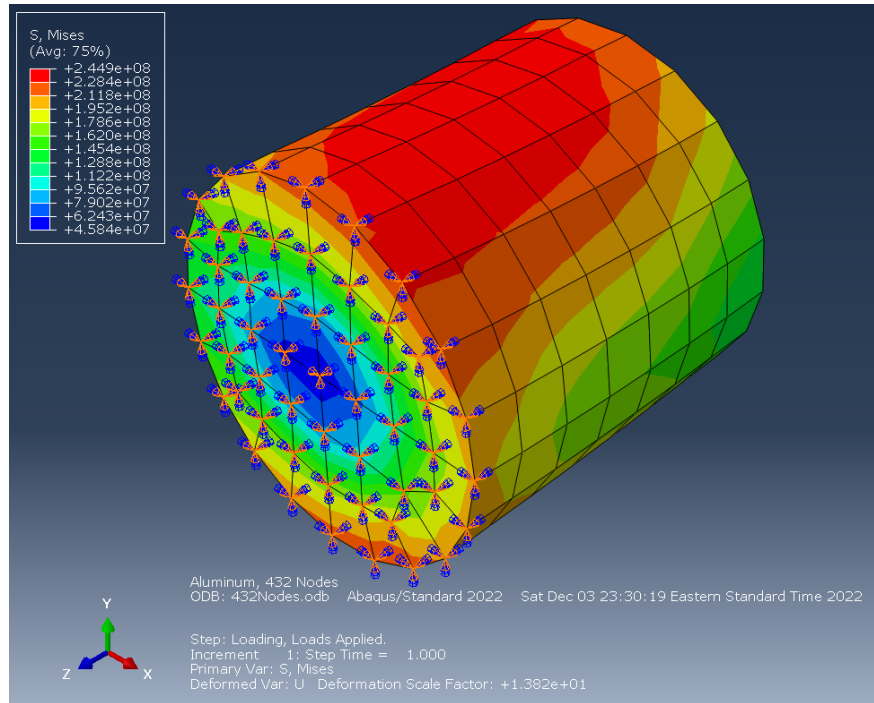


Fig. 6. Aluminum simulation with von Mises stress results contour plot [1].

5.

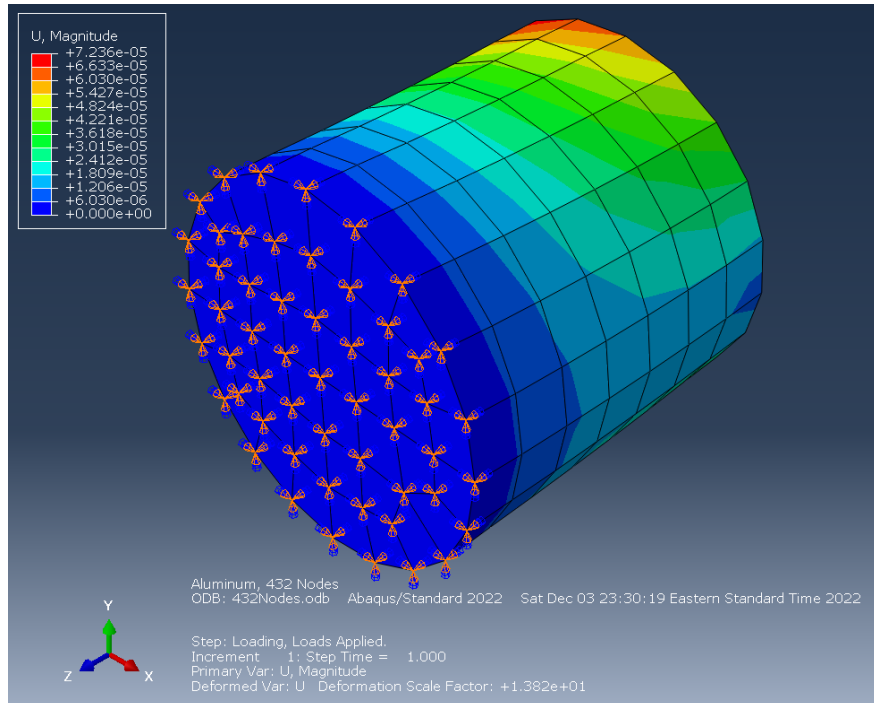


Fig. 7. Aluminum simulation with deformation contour plot; face with fixed circular front [1].

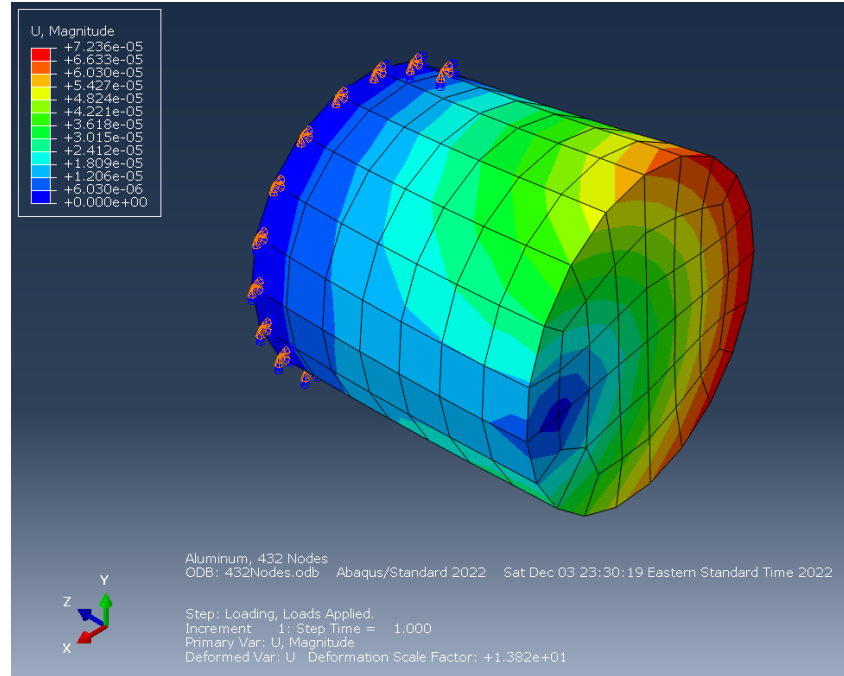


Fig. 8. Aluminum simulation with deformation contour plot; face with applied load front [1].

6.

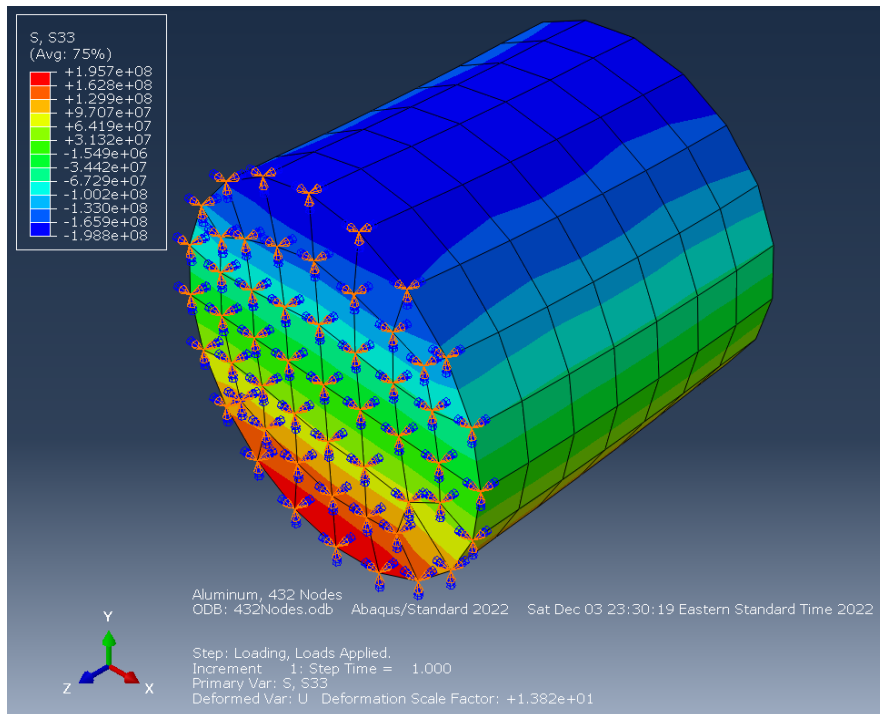


Fig. 9. Aluminum simulation with S33 stress plot [1].

7.

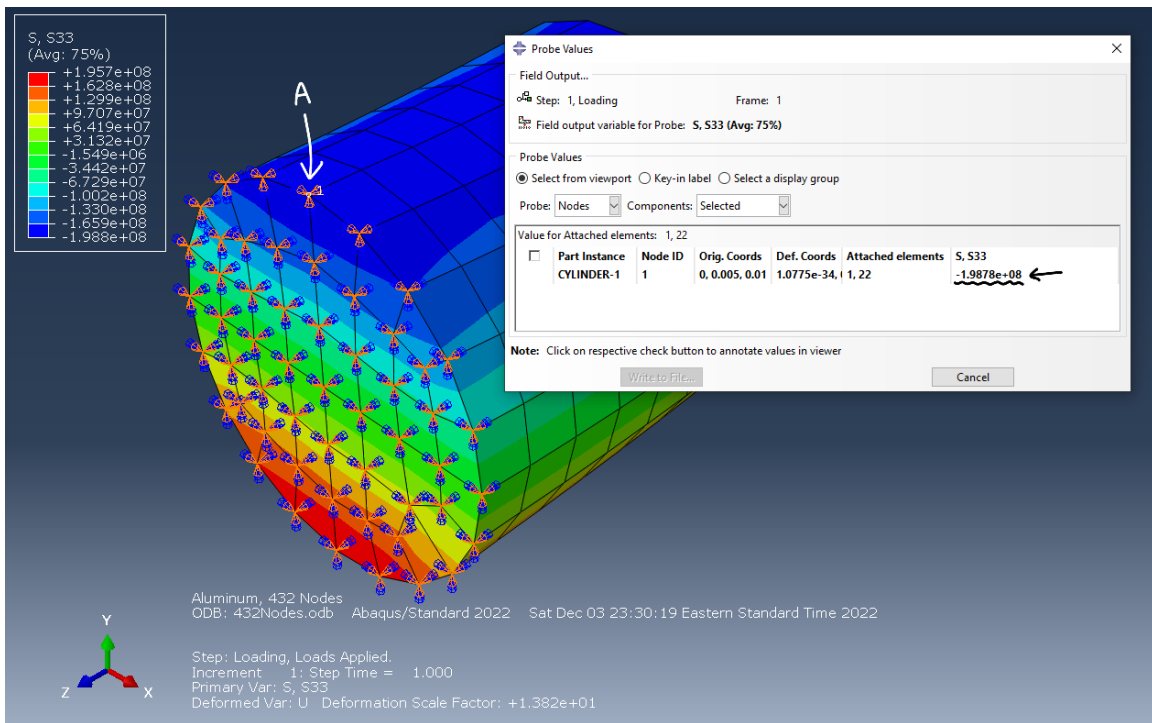


Fig. 10. S33 stress values for point A [1].

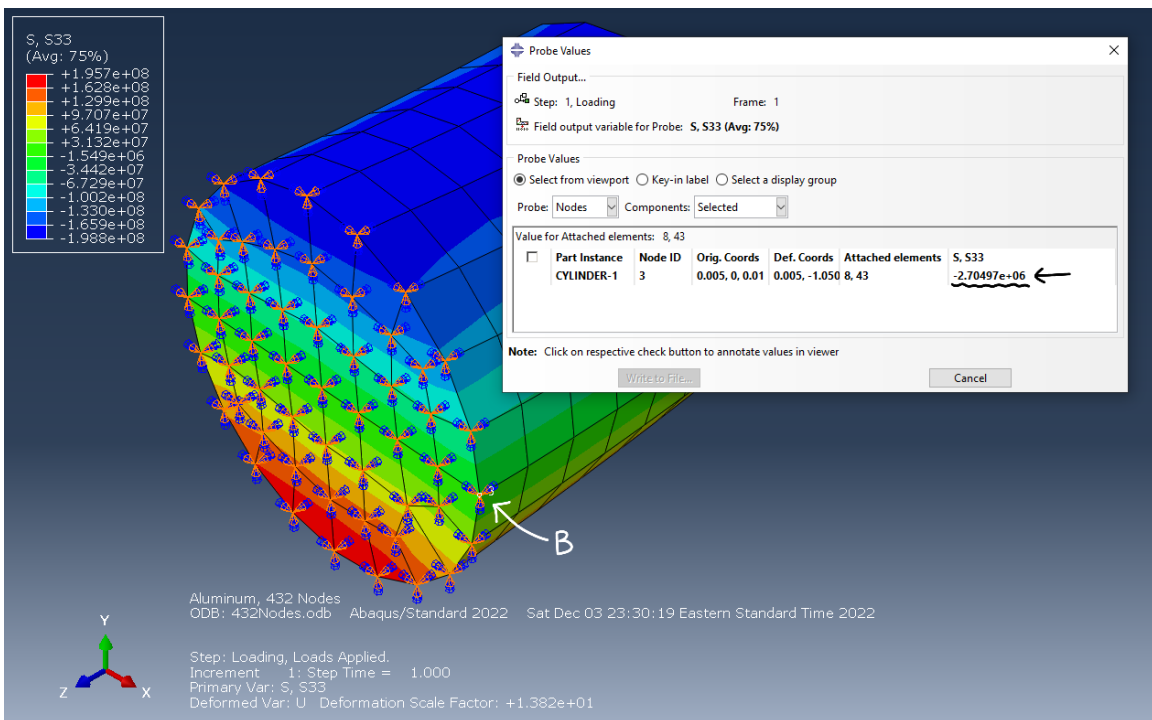


Fig. 11. S33 stress values for point B [1].

8.

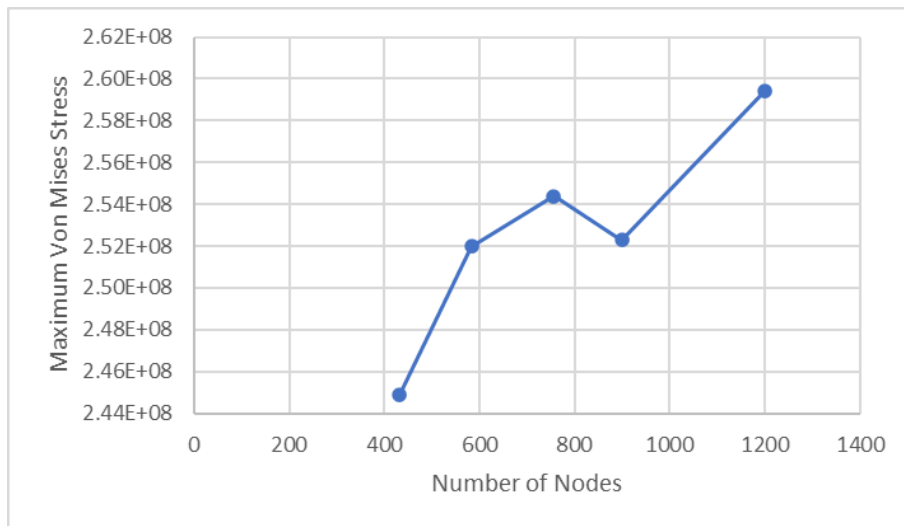


Fig. 12. Number of nodes vs. maximum von Mises stress plot.

9.

Table II

Comparing Hand-Calculated and Simulated S33 Stress Values for Points A and B [1]

	Point A	Point B
Hand Calculated Stress	-2.15×10^8 Pa	-1.53×10^6 Pa
Probed Stress Values	-2.14×10^8 Pa	-1.21×10^6 Pa
Percent Error	0.26%	21.19%

10.

Table III

Comparing Hand-Calculated, Aluminum-Simulated, and Steel-Simulated S33 Stress Values for Points A and B [1]

Calculation	Point A	Point B
Hand Calculation	-4.29×10^8 Pa	-1.53×10^6 Pa
Aluminum Simulation	-2.14445×10^8 Pa	-1.20583×10^6 Pa
Steel Simulation	-2.1413×10^8 Pa	-1.19292×10^8 Pa

III. Discussion

1. The addition of a coupling constraint ensured that nodes on the same surface of the reference point were constrained to the rigid-body motion of the reference node. Without the coupling constraint, the applied load T would solely impact the reference node rather than the entire surface [2]. This, in turn, would yield wildly inaccurate results given that the motor twisted the entire drill, not a singular point at the centre of its cross section.
2. In the pre-lab exercise, M acting on the fixed surface containing points A and B uses 400 mm as its distance, disregarding the 10 mm distance between the cross-section and reference-node-containing surface where the loads are applied. The internal force values are disrupted as a result. By using 390 mm instead, the internal forces are left unaffected by M , and thus, exhibit greater accuracy. These adjusted loads are displayed in Fig. 13.

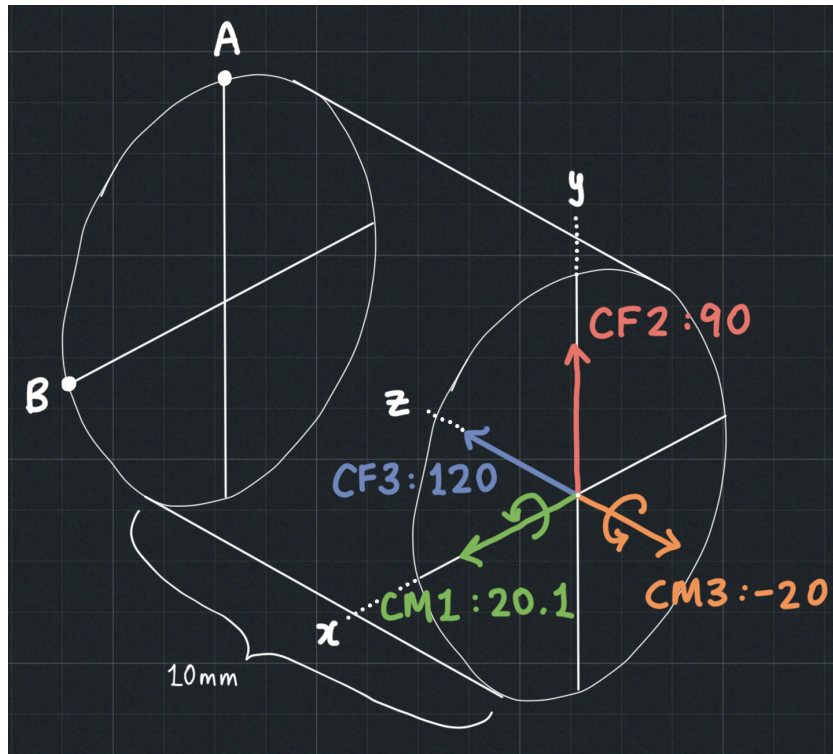


Fig. 13. Adjusted loads for a 10 mm difference.

3. Partitioning the cylindrical face prior to meshing generated more consistent element sizes (see Fig. 14) as opposed to the more distorted elements when no partitions were carried out (see Fig. 15). Although deformation is no cause for concern, all elements have a

particular range of allowable distortion [3], and once this range is exceeded, degeneration is triggered, whereby elements collapse by one or more edge [4]. Notwithstanding that such degeneration has its uses, in the context of this lab, it produces erroneous data by understating the effects of deformation to the model [3]. Consequently, the simplification of more complex geometries via partitioning is essential for maximizing accuracy.

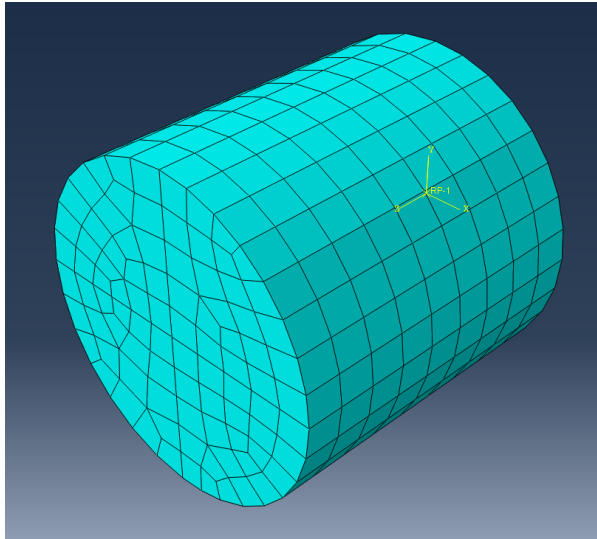


Fig. 14. Meshed after partitioning [1].

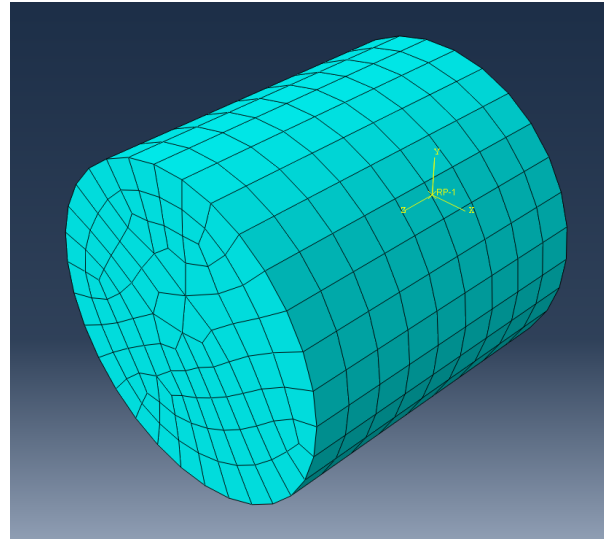


Fig. 15. Meshed with no partition [1].

4. Mesh convergence is a process by which the element size necessary for simulated data to be unaffected by mesh size is determined [5]. It is exemplified through Fig. 12, where the behaviour of the maximum von Mises stress was graphed as the number of nodes was modified. Mesh size displays the most convergence at the intervals where the least change is observed in the von Mises stress [6]; upon inspection of the plot, this is most present at about 700 nodes. Additionally, the graph indicates that a significantly high mesh size (i.e., lesser number of nodes) worsens the accuracy just as much as a significantly low mesh size (i.e., greater number of nodes) does [7].

5. S33 values represent the stresses occurring along the z-axis [8]. While von Mises stresses are a theoretical measure of stress used for approximating the failure criteria for yielding, principal stresses are much more tangible and measurable, signifying the maximum (or minimum) normal stresses developed on planes of a loaded body with no shear stresses [9].

6. As shown in Table 2, the hand-calculated stress values are near-equivalent to the simulated stress values at point A, but are fairly dissimilar at point B. The discrepancy in percent error would have to be a result of the position of the points in relation to the neutral axis. Whereas point B is located directly on the neutral axis, point A is 5 mm above it, directly affecting the bending stress term (i.e., My/I) in the summation of S33 stresses (i.e., normal stresses in the z-direction) at both points. Hence, it is presumed that Abaqus [1] did not treat the node representing point B as being directly on the neutral axis, but rather, some distance above or below it. This would create a non-zero bending stress, and thus, affect the magnitude of the total S33 stress [9].

7. The stress distribution of the cylinder does not depend on the material since fundamentally, neither normal nor shear stresses depend on variables that are intrinsic to certain materials, like Young's modulus. Rather, the variables and their relationships to one another depend on applied loads (e.g. N and V), moments (e.g., M and T), and geometric properties (e.g., cross-sectional area, distances from neutral axes, area and polar moments of inertia, radius of curvature, etc.), all three of which are unrelated to the material in question. As long as the cylinder remains a cylinder, and the forces and moments applied to it remain the same, no significant dependence is plausible [9]. Comparing the S33 stresses for the aluminum and steel simulations listed in Table 3 further validate the argument, with the values being roughly the same.

8. Drill bits should possess strong rigidity since their usage involves withstanding contact forces and moments from the material's surface and drill motor. If the drill bit deforms, the final hole may turn out more jagged and splintered than initially intended, not turn out at all, or break the drill itself. Fig. 16 and 17 reveal that aluminum has a much higher maximum deformation compared to steel, with the latter showing three times more rigidity than the former. Therefore, in the application of drill bits, steel is the material of choice.

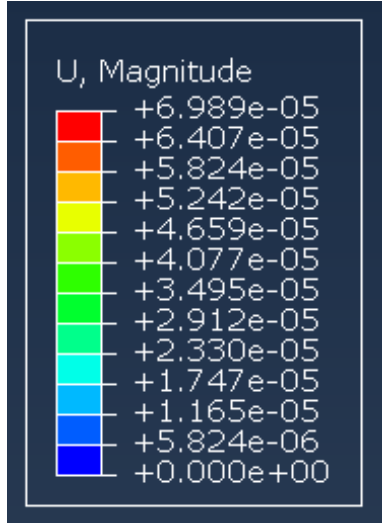


Fig. 16. Deformation values for aluminum [1].

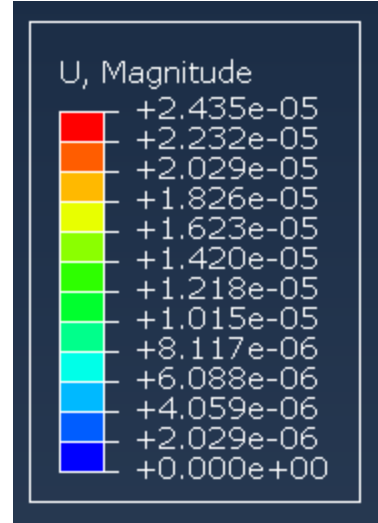


Fig. 17. Deformation values for steel [1].

9. Given that the meniscus experiences forces and moments from the body's weight, the boundary conditions would be set on the bottom surface of the Abaqus model [1]. As there are two points of contact between the femur and meniscus (i.e., one on the medial and lateral each), the load-defining reference nodes would be defined approximately at the centroids of the top surfaces of each meniscus. The stress from the femur would be divided between the two menisci. Notably, the load types and magnitudes would vary depending on the flexion of the knee when landing the jump. Consequently, one must consider the muscles dampening the impact of the jump as well. With zero flexion, however, there is no muscle dampening, and only N acts on the meniscus. Assuming the body is landing from a jump height of 25 cm, the normal force on each reference node would be approximately 1757 N using the average body mass index (see Fig. 18) [10]. With a flexion of angle Θ , N would be $1757\cos\Theta$ N, and V would be $1757\sin\Theta$ N, assuming no muscle dampening (see Fig. 19). M would depend on the force component from the weight of the upper body, as well as the length of the femur and flexion angle (see Fig. 20). There is no T applied to the meniscus.

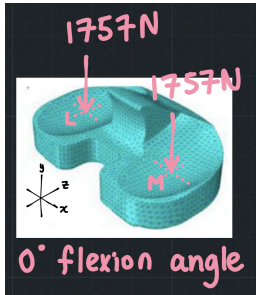


Fig. 18. N with no flexion of the knee.

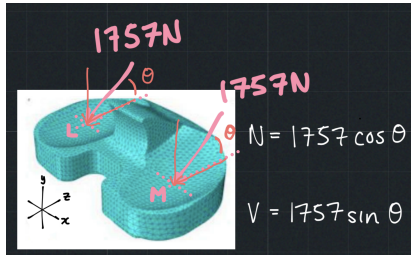


Fig. 19. N and V with flexion angle θ .

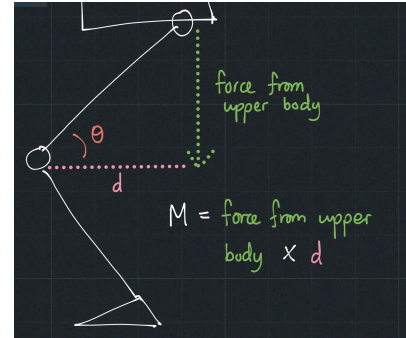


Fig. 20. M with flexion of the knee.

10. FEA provides a comprehensive set of results with several failure modes while simultaneously eliminating the need for physical prototypes in the event that they are especially costly, slow down the workflow, or simply inefficient all-around. Nonetheless, limitations missing in experimental testing were noted. For one, all of its computations and subsequent solutions are approximate, and due in part to the limited number of digits any computer is capable of holding, round-off errors are inevitable. Bugs and software malfunctions are likewise inevitable, and can likewise skew data accuracy. Oftentimes, FEA software developers will exploit these general issues by charging users extra for improved computer memory, running times, and IT support. Furthermore, it was made apparent that the final plots varied drastically from job to job despite the conditions remaining unchanged; this was later determined to be a consequence of meshing. FEA analysis is also not particularly beginner-friendly, requiring a strong foundation in the mechanics of materials as well as a sound engineering judgement. This steep learning curve can easily sway new users away.

IV. Conclusion

Ultimately, the FEA software, Abaqus [1], is an efficient software to use in engineering when physical prototypes are unreasonable to purchase. With proper engineering judgement, Abaqus is able to provide approximate results and allows engineers to understand the different forces that come into play with different members. A simple error made which was immediately

corrected was including a negative sign before 120 instead of a positive value for CM3. This was noticed after re-checking work, and was almost immediately found. As explicitly explained in the discussion, improvements to this study can be made through partitioning the cylindrical face prior to meshing due to being able to generate more consistent element sizes. It was hypothesised that the hand-calculated results would be similar to Abaqus [1]. Although the hand-calculated stress values are similar to the simulated stress values at point A, they are dissimilar at point B as a result of the position of the points in relation to the neutral axis. All in all, although it is possible to use FEA softwares such as Abaqus to find stress values, hand-calculations of these values are shown to be more accurate.

References

- [1] “Abaqus learning edition,” *3DEXPERIENCE EDU*. [Online]. Available: <https://edu.3ds.com/en/software/abaqus-learning-edition>. [Accessed: 04-Dec-2022].
- [2] “28.3.2 Coupling constraints,” *Abaqus Analysis User's manual (V6.6)*. [Online]. Available: <https://classes.engineering.wustl.edu/2009/spring/mase5513/abaqus/docs/v6.6/books/usb/default.htm?startat=pt08ch28s03aus108.html>. [Accessed: 03-Dec-2022].
- [3] “Mesh quality parameters in finite element analysis,” EngMorph. [Online]. Available: <https://www.engmorph.com/mesh-quality-parameters>. [Accessed: 04-Dec-2022].
- [4] “Element degeneration,” Altair Radioss. [Online]. Available: https://2021.help.altair.com/2021/hwsolvers/rad/topics/solvers/rad/theory_element_element_degeneration_r.htm. [Accessed: 03-Dec-2022].
- [5] NAFEMS, “The Importance of Mesh Convergence,” The importance of Mesh Convergence. [Online]. Available: <https://www.nafems.org/publications/knowledge-base/the-importance-of-mesh-convergence-part-1/>. [Accessed: 03-Dec-2022].
- [6] J. VanWagnen, “Element size in FEA - does it matter?,” Fidelis, 09-Sep-2021. [Online]. Available: <https://www.fidelisfea.com/post/element-size-infea-does-it-matter>. [Accessed: 03-Dec-2022].
- [7] R. Omar, M. N. Abdul Rani, M. A. Yunus, A. A. Mat Isa, W. I. Wan Iskandar Mirza, M. S. Mohd Zin, and L. Roslan, “Investigation of mesh size effect on dynamic behaviour of an

- assembled structure with bolted joints using finite element method," International Journal of Automotive and Mechanical Engineering, vol. 15, no. 3, pp. 5695–5708, 2018.
- [8] E. V. Arcieri, S. Baragetti, and M. Lavella, "Effects of FOD on fatigue strength of 7075-T6 hourglass specimens," IOP Conference Series: Materials Science and Engineering, vol. 1038, no. 1, p. 012012, 2021.
- [9] R. C. Hibbeler and K. B. Yap, Mechanics of Materials, 10th ed. Harlow: Pearson, 2018.
- [10] M. D. Makinejad, N. A. Abu Osman, W. A. Wan Abas, and M. Bayat, "Preliminary analysis of knee stress in full extension landing," *Clinics*, vol. 68, no. 9, pp. 1180–1188, Sep. 2013.